Correspondence Between Trichome Morphology and Phylogenetic Distance in Six Solanaceae Species

HyunShin Lee
Chungnam Science High School

ABSTRACT

Trichomes are highly diverse epidermal appendages, but their phylogenetic utility remains insufficiently tested in a quantitative framework. This study evaluated whether quantitative trichome morphology corresponds to molecular phylogenetic distance in six Solanaceae species. Twenty-six quantitative traits were measured from scanning electron micrographs, and a focal trait block composed of Tortuosity, Mean Curvature, and Curvature per Length was prioritized for analysis. Species-level morphological distances were calculated from standardized trait values and compared with patristic distances derived from an *rbcL*- and *matK*-based phylogeny using exact Mantel tests. The focal trait block showed significant positive correlation with molecular distance (Spearman r_M = 0.775, p = 0.044; Pearson r_M = 0.865, p = 0.046). Although principal component analysis did not produce complete visual separation among all species, the distance-matrix comparison showed concordant variation between trichome morphology and molecular phylogeny. Sensitivity analysis further showed that adding Contraction Ratio weakened the correspondence. These results indicate that the focal path-curvature trait block captures a limited but significant matrix-level phylogenetic signal in the six Solanaceae species examined, although a robust morphology-based classification system has not yet been established.

KEYWORDS

Trichome, Phylogenetic, Quantitative morphology, Curvature, Mantel tests

1. INTRODUCTION

1.1. Research Background and Necessity

Trichomes are specialized epidermal appendages that exhibit substantial diversity in morphology, distribution, composition, and function. They play multiple roles on the plant surface, including physical defense, secretion, regulation of transpiration, and interactions with the external environment, and therefore provide important clues for understanding plant survival strategies and adaptive responses[1-2].

However, much of the previous research on trichomes has focused on morphological descriptions at the level of individual species or limited genera, on the distinction between glandular and nonglandular trichomes, or on the interpretation of specific functions. Although such approaches are useful for describing the characteristics of individual taxa, they are limited in their ability to test which morphological traits actually reflect phylogenetic differences among species. Even in comparative studies involving multiple species, conventional traits such as length, width, and branch number have frequently been used; however, these variables alone are insufficient to explain the overall structure and organization of trichomes. Even superficially similar trichomes may differ substantially in the trajectory of the central axis, the pattern of curvature, and the cumulative curvature relative to length. For this reason, trichome morphology should be evaluated not only in terms of size or count-based descriptors, but also in terms of structural path geometry and curvature.

The present study quantitatively analyzed trichomes of six Solanaceae species and compared the resulting morphological distance matrix with a molecular distance matrix derived from an *rbcL*- and *matK*-based phylogeny using the Mantel test. Through this approach, the study aimed to reassess the phylogenetic utility of trichome

morphology. In particular, the study is meaningful in that multiple quantitative traits capable of representing overall trichome structure were measured, and a subset of traits suitable for interspecific comparison and structural interpretation was subsequently selected for focused analysis.

1.2. Objectives of the Study

The objective of this study was to construct a morphological distance matrix from measurable quantitative trichome traits in six Solanaceae species and to compare it with a molecular distance matrix derived from an *rbcL*- and *matK*-based phylogeny in order to evaluate the phylogenetic relevance of trichome morphology.

To achieve this objective, the study addressed the following three questions. First, do trichomes of the six Solanaceae species differ at the level of quantitative traits? Second, can a focal trait block prioritized on structural and technical grounds provide an informative representation of interspecific morphological distance structure? Third, does the resulting morphological distance matrix show significant correspondence with the molecular phylogenetic distance matrix?

By addressing these questions, this study aims not to exhaustively optimize among all possible trait combinations, but to evaluate whether a structurally interpretable focal block can capture phylogenetically relevant variation in Solanaceae trichomes and provide a basis for more refined follow-up studies.

1.3. Significance of the Study

First, this study treats trichomes of Solanaceae not simply as qualitatively described surface structures, but as a set of structurally quantifiable traits. This reduces reliance on impressionistic interpretation and improves the comparability of morphological information across taxa.

Second, this study evaluates trichome-based phylogenetic signal through the direct comparison of a morphological distance matrix and a molecular phylogenetic distance matrix using an exact Mantel test. In this respect, the study is methodologically meaningful because it distinguishes visual cluster separation from statistical correspondence.

Third, the study proposes a focal trait block and an analytical framework that may reveal phylogenetically relevant variation in Solanaceae trichomes. Its significance lies not in presenting a fully resolved morphology-based classification system, but in clarifying how trichome traits may be selected, interpreted, and tested in a matrix-based comparative framework.

2. THEORETICAL BACKGROUND

2.1. Classification of Trichomes

Trichomes may be broadly classified, on the basis of morphology and surface appearance, into pubescent forms and glaucous forms, the latter being covered with wax and showing a bluish or whitish appearance [3]. More specifically, trichomes have been subdivided into categories such as arachnoid, canescent, hirsute, hispid, lanate, pilose, puberulent, scabrous, sericeous, strigose, and tomentose [3]. Trichomes may be unicellular or multicellular and may occur singly or in tufts [3]. They may also be classified according to branching pattern and according to the presence or absence of secretion, that is, into nonglandular and glandular trichomes.

2.2. Functions of Trichomes

Trichomes perform diverse functions that parallel their morphological diversity. In general, trichomes protect plants from environmental stressors such as herbivores, pathogens, and frost through both physical and chemical defense mechanisms [4]. Some glandular trichomes act as biological microfactories by synthesizing and secreting a wide range of bioactive compounds and metabolites, thereby playing important roles in plant defense and metabolism [4]. However, trichomes do not serve identical functions in all plant species, and their functional roles differ among taxa [2–3].

2.3. Morphological, Quantitative, and Qualitative Traits

Morphological traits are observable external characteristics of plants and are among the most widely used sources of evidence in plant identification and classification. Such traits provide essential information for inferring phylogenetic relationships and may be observed in both vegetative and reproductive organs [3]. In the present study, trichomes on the plant epidermis were treated as morphological characters of interest.

Morphological characters may be divided into quantitative and qualitative traits. Quantitative traits are continuous variables that can be expressed numerically, such as length, width, or mass. By contrast, qualitative traits are discrete or categorical states, such as presence or absence, shape class, or branching type. Because quantitative traits allow direct measurement and numerical comparison, they are particularly useful when interspecific differences must be translated into distance-based matrices for statistical comparison.

2.4. Homology and Analogy: Definitions and Significance

Similarity derived from common ancestry is referred to as homology, whereas similarity produced by convergent evolution is referred to as analogy [6]. Homology implies that a particular character state was present in a common ancestor and subsequently diversified under different environmental conditions in descendant lineages. Analogy, in contrast, refers to similarity in form or function that is not derived from a shared ancestral origin. In general, when similar traits are observed among distantly related lineages, those similarities are more likely to represent analogy than homology.

This distinction is important in morphological studies because external similarity alone does not guarantee phylogenetic relatedness. A trait can be morphologically similar across taxa while differing in evolutionary origin. Therefore, the phylogenetic interpretation of trichome morphology requires explicit comparison with an independent phylogenetic framework.

2.5. Significance of Trichomes as Phylogenetically Informative Characters

Trichomes exhibit remarkable diversity. More than 21 trichome types have been reported, and in the genus Solanum alone, 57 types have been described [1]. This extensive diversity makes rigorous systematic classification difficult [2], but at the same time it may increase the phylogenetic utility of trichomes. In other words, the broad variation in trichome morphology and composition, although taxonomically complex, may also provide a rich pool of potentially informative characters for phylogenetic comparison.

For this reason, trichomes should not be treated merely as superficial surface structures. Instead, they may be considered candidate morphological characters that could preserve phylogenetic information when appropriately measured and analyzed.

2.6. Molecular Phylogenetic Trees and the *rbcL* and *matK* Markers

Molecular phylogenetic trees are among the most widely used tools in modern systematics for inferring evolutionary relationships. Because they reflect shared ancestry more directly than morphology alone, they provide an objective basis for reconstructing evolutionary history [7].

The *rbcL* gene encodes a subunit of the photosynthetic enzyme Ribulose-1,5-bisphosphate carboxylase/oxygenase and is relatively slow-evolving and highly conserved. For this reason, it is useful for resolving phylogenetic distances among higher-level taxa such as families and genera. By contrast, the *matK* gene evolves more rapidly than rbcL and exhibits more frequent sequence variation, making it more useful for distinguishing closely related species [7].

Accordingly, the combination of rbcL and matK provides a suitable molecular reference phylogeny for comparison with morphological characters. In this study, these markers were not used to identify genes directly involved in trichome development, but rather to provide an independent phylogenetic framework against which trichome-based morphological distances could be evaluated.

2.7. Theoretical Significance of Path-Curvature Traits

Traditional descriptors such as length, width, and branch number provide useful information about trichome morphology, but they do not fully describe the structural organization of the entire trichome. Even when two trichomes have similar overall size or branch number, they may differ substantially in the trajectory of the central axis, the degree of bending, and the cumulative curvature distributed along the structure. For this reason, trichome morphology should be interpreted not only in terms of size, but also in terms of path geometry and curvature.

From this perspective, traits related to path and curvature may provide more direct information on overall structural organization than conventional size-based descriptors. Tortuosity reflects how strongly a trichome axis deviates from a straight path. Mean curvature summarizes the average degree of bending along the axis. A length-normalized curvature metric can further reduce the confounding effect of absolute size by evaluating cumulative curvature relative to total length. Together, such traits provide a theoretical basis for examining whether structural geometry, rather than size alone, better captures phylogenetically meaningful variation.

2.8. Mantel test

Studies that use morphological traits for phylogenetic interpretation often face two major problems. First, morphological traits may be influenced by environmental conditions, developmental stage, imaging resolution, and measurement procedures, and are therefore often regarded as less stable than molecular data. Second, even when morphology is quantified, the resulting patterns are often interpreted descriptively without sufficiently testing which traits actually reflect interspecific phylogenetic relationships. As a result, the statement that two taxa "look different" is often conflated with the claim that the difference is phylogenetically meaningful.

To address this problem, morphological data must be organized in a form that can be directly compared with molecular data. In the present context, the relevant research question is not how clearly taxa separate in a visualization space, but how strongly the structure of interspecific morphological distances corresponds to the structure of interspecific molecular distances. The Mantel test is methodologically well suited to this purpose because it evaluates the overall correspondence between two distance matrices after reducing both morphology and molecular data to comparable matrix structures [5].

Thus, the Mantel test provides an appropriate framework for assessing whether variation in trichome morphology is merely descriptive or whether it shows a statistically detectable relationship with molecular phylogenetic distance.

3. RESEARCH METHODS AND PROCEDURES

3.1. Study Species

This study was conducted on six trichome-bearing species in Solanaceae (Table 1): *Brugmansia suaveolens*, *Capsicum annuum* L. var. grossum, *Lycium chinense* Mill., *Petunia* × *hybrida* 'Dreams Red', *Physalis alkekengi* L. var. franchetii, and *Solanum nigrum* L. The study plants were obtained either by purchase or collection, and the presence of trichomes was confirmed in all species using a light microscope prior to analysis. Thereafter, all plants were cultivated under identical growth-chamber conditions: 70% relative humidity, a light intensity of 10,000 lx, a 12-h photoperiod, and a temperature of 20°C.

The habitat conditions of the six Solanaceae species were as follows. *Brugmansia suaveolens* occurs in humid lowland regions under tropical climates. *Capsicum annuum* var. grossum, *Physalis alkekengi* var. franchetii, and *Solanum nigrum* occur in humid lowland regions under subtropical to tropical climates. *Lycium chinense* Mill. is distributed in dry lowland regions under temperate climates, whereas *Petunia* × *hybrida* 'Dreams Red' occurs in humid lowland regions under tropical climates.

Family	Study Species
Solanaceae	*Brugmansia suaveolens*
	Capsicum annuum L. var. Grossum
	Lycium chinense Mill.
	Petunia × *hybrida* 'Dreams Red'
	Physalis alkekengi L. var. franchetii
	Solanum nigrum L.

Table 1. Study Species Used in This Study. List of the six Solanaceae species included in this study. All species were confirmed to bear trichomes prior to analysis and were used for both morphological quantification and molecular phylogenetic comparison.

3.2. Observation and Imaging of Trichomes Using SEM

Leaf regions bearing trichomes were excised into pieces of approximately 1 cm^2. For scanning electron microscope (SEM) observation, the samples were dehydrated by sequential immersion for 15 min each in aqueous ethanol solutions of increasing concentration (30%, 50%, 60%, 70%, 80%, 90%, 95%, and 100%). The dehydrated samples were then immersed in tert-butanol to replace the ethanol within the tissues, followed by overnight drying in a freeze dryer. After drying, the samples were gold-coated using a plasma coater. For each species, at least 30 SEM images of trichomes were observed and recorded.

3.3. Measurement of Quantitative Traits of Trichomes

Basic geometric dimensions required for downstream quantification were first obtained from SEM images using ImageJ. To quantify traits that were difficult to obtain directly in ImageJ, trichome recognition and detection were performed in Python 3 using the NumPy, OpenCV, SciPy, and Matplotlib libraries. Flood fill, Otsu's binarization, GrabCut, and contour detection algorithms were used for trichome extraction and image segmentation. Subsequently, polynomial operations, skeletonization, distance transform, convex hull construction, ellipse fitting, breadth-first search, and vector operations were applied to derive 26 quantitative traits for downstream analysis.

Quantitative Trait	unit
Area	μm^2
Perimeter	μm
Bounding Box Aspect Ratio	ratio
Ellipse Major Axis	μm
Ellipse Minor Axis	μm
Ellipse Angle	degree
Contraction Ratio	ratio
Number of Endpoints	count
Number of Branchpoints	count
Length	μm
Straight Length	μm
Tortuosity	ratio
Width (Base)	μm
Width (Tip)	μm
Width (Max)	μm
Mean Curvature	rad
Max Curvature	rad
Sum of Curvature	rad
Skeleton Length	μm
Skeleton Ratio	ratio
Mean Upper Curvature Traits	rad
Max Upper Curvature Traits	rad
Sum Upper Curvature Traits	rad
Mean Lower Curvature Traits	rad
Max Lower Curvature Traits	rad
Sum Lower Curvature Traits	rad

Table 2. Quantitative Traits Measured From Trichome Images List of the 26 quantitative traits measured from SEM images and image-processing analyses. These traits include size-related variables, axis-based path variables, curvature-related variables, branching variables, and skeleton-based variables. Among them, Tortuosity, Mean Curvature, and Curvature per Length were selected as the focal traits for the main analysis, whereas Contraction Ratio was retained only for sensitivity analysis.

3.4. Verification of Normality and Statistical Significance of Quantitative Traits

To examine the distributional properties of the measured quantitative traits, the Shapiro–Wilk test was performed (1). The results indicated that most of the quantitative-trait data did not satisfy normality. Accordingly, the Kruskal–Wallis test was used to examine exploratory interspecific differences at the level of individual traits (2).

$$W = \frac{\left(\sum_{i=1}^{n} a_i x_{(i)}\right)^2}{\sum_{i=1}^{n}(x_i - \bar{x})^2} \qquad (1)$$

W denotes the Shapiro–Wilk test statistic, where values closer to 1 indicate closer agreement with a normal distribution; x_i denotes the i -th ordered sample value; $\bar{x}$ denotes the sample mean; and ai denotes a constant derived from the order statistics of a normal distribution.

$$H = \frac{12}{N(N+1)} \sum_{i=1}^{k} \frac{R_i^2}{n_i} - 3(N+1) \qquad (2)$$

H denotes the Kruskal–Wallis test statistic, which is approximately chi-squared distributed; N denotes the total number of observations; k denotes the number of groups being compared; n_i denotes the sample size of the i-th group; and R_i denotes the sum of ranks for observations in the i-th group.

In the present study, these tests were used as diagnostic procedures rather than as the sole basis for focal trait selection. Because the main objective was to evaluate morphology–molecular correspondence at the level of distance-matrix structure, focal trait selection was determined by combining structural interpretability, reduced size dominance, limited redundancy among core dimensions, and matrix-level suitability, rather than by relying only on univariate significance.

3.5. Selection of Target Quantitative Traits

Because not all measured quantitative traits were equally suitable for interspecific similarity calculation or morphology-based phylogenetic comparison, a focal set of quantitative traits was prioritized from the 26 measured variables. Trait selection was not based solely on univariate statistical significance. Instead, traits were evaluated according to four criteria: structural interpretability, reduced dominance by absolute size, limited redundancy among core dimensions, and suitability for matrix-level comparison.

On this basis, Tortuosity, Mean Curvature, and Curvature per Length were selected as the focal quantitative traits for the main analysis. Tortuosity represents path deviation from a straight trajectory, Mean Curvature summarizes overall bending of the central axis, and Curvature per Length, defined as Sum of Curvature divided by Length, provides a length-normalized measure of cumulative curvature. This last variable was used instead of Sum of Curvature alone because the latter may reflect absolute size as well as curvature itself in interspecific comparisons. Contraction Ratio was retained only as an auxiliary variable for sensitivity analysis. To remove directional information while preserving magnitude, the absolute value of Contraction Ratio was taken and then log-transformed. It was therefore treated as a supplementary variable rather than as part of the focal trait block.

By contrast, size-dominant descriptors such as Area, Perimeter, Length, Straight Length, Width (Base), Width (Tip), Width (Max), Ellipse Major Axis, Ellipse Minor Axis, and Skeleton Length were not prioritized as focal traits. Under the present dataset, these variables were strongly associated with a common size axis and were therefore considered more likely to reflect overall scale than structural organization.

Orientation-sensitive variables such as Bounding Box Aspect Ratio and Ellipse Angle were likewise not prioritized as focal traits. These variables may change according to image orientation and projection in two-

dimensional representations. However, because the present study did not include explicit image-rotation perturbation tests, this exclusion should be interpreted as methodologically motivated but only partially validated under the current tabular dataset.

Among curvature-related variables, Max Curvature and the Upper and Lower Curvature traits were not prioritized because they depend more strongly on local extrema or partial segments than on whole-axis structure. These variables may therefore be more sensitive to local image noise or segmentation instability than Mean Curvature, which summarizes curvature across the full axis. As with the orientation-sensitive variables, this rationale is conceptually strong but remains only partially validated without image-based perturbation tests.

Finally, Skeleton Ratio was not prioritized as a focal trait. Although it contains information related to path complexity, the present dataset suggested that it provided less direct structural interpretation than the focal path–curvature traits and less added value for matrix-level comparison than the selected block.

In summary, interspecific morphological comparison and distance-matrix construction in the present study were based primarily on the focal traits Tortuosity, Mean Curvature, and Curvature per Length, whereas Contraction Ratio was used only in sensitivity analysis. The empirical evaluation of this prioritization and exclusion logic is presented in the Results section.

3.6. Construction of the Morphological Distance Matrix for the Mantel Test

The species-level representative matrix of the focal quantitative traits was standardized using z-scores in order to remove differences in units among traits. Euclidean distance was then used to calculate pairwise morphological distances among species (3), thereby generating the morphological distance matrix.

$$d_{ij}^{morph} = \sqrt{\sum_{k=1}^{p} \left(z_{ik} - z_{jk}\right)^2} \qquad (3)$$

d_{ij}^{morph} denotes the morphological distance between species *i* and *j*; *p* denotes the total number of morphological traits used for the calculation; *k* denotes the index of an individual trait; and z_{ik} and z_{jk} denote the z-score standardized values of the *k*-th trait for species *i* and species *j*, respectively.

3.7. Construction of the Molecular Distance Matrix Based on rbcL and matK Sequences

FASTA sequences of *rbcL* and *matK* for the study species were collected from NCBI GenBank. Multiple sequence alignment was performed separately for each gene using Clustal Omega, after which the two alignments were concatenated into a supermatrix. A phylogenetic tree was then inferred using IQ-TREE, and branch support was evaluated with 1,000 replicates each of SH-aLRT and Ultrafast Bootstrap. Patristic distances, defined as the sums of branch lengths between pairs of taxa, were then calculated from the resulting phylogeny to construct the molecular distance matrix based on *rbcL* and *matK*.

3.8. Mantel Test Comparing the Morphological Distance Matrix with the Molecular Distance Matrix

The correspondence between the morphological distance matrix and the molecular distance matrix was evaluated using the Mantel test in order to assess morphology–molecular correspondence. First, the upper-triangular elements of the two distance matrices were vectorized and paired, and correlation coefficients were calculated between the two vectors. The rank-based Spearman Mantel test was used as the primary test, and the Pearson Mantel test was conducted as a supplementary analysis.

The Spearman test was adopted as the main inferential criterion because it is appropriate for evaluating concordance in the rank order of distances rather than only the absolute values of distances. The Pearson test was used as a supplementary indicator of linear correspondence between distance values.

Because the study included only six Solanaceae species, an exact permutation approach was used instead of approximate randomization. Specifically, all possible permutations of species labels (6! = 720) were exhaustively evaluated to construct the null distribution of the Mantel correlation coefficient, from which exact p-values were obtained. This approach was intended to provide a more conservative and rigorous assessment of significance for a small sample.

Principal component analysis was used as a descriptive visualization of morphospace. Hierarchical clustering was examined only as a supplementary topology check and was not treated as a primary source of phylogenetic inference. Statistical inference regarding morphology–molecular correspondence was based on the exact Mantel test.

3.9. Sensitivity Analysis

Sensitivity analysis was performed to determine whether the morphology–molecular correspondence derived from the focal trait block depended excessively on a particular species or on a particular choice of traits.

First, a leave-one-species-out analysis was conducted. One species at a time was excluded from the six-species dataset, and the morphological and molecular distance matrices were recalculated for the remaining five species. Exact Mantel tests were then repeated for each reduced dataset. This procedure was used to evaluate the structural stability of the observed morphology–molecular correspondence with respect to species composition.

Second, the auxiliary contribution of Contraction Ratio was examined. Although Contraction Ratio was considered unstable as a focal trait because it contains both directional and magnitude information, it was not excluded entirely because it may still reflect structural contraction to some extent. Instead, it was evaluated separately at the sensitivity-analysis stage. An expanded trait block was constructed by adding contraction_abs to the focal block composed of Tortuosity, Mean Curvature, and Curvature per Length. The morphological distance matrix was then recalculated, and an exact Mantel test was performed between the expanded morphological distance matrix and the molecular distance matrix to evaluate whether the inclusion of Contraction Ratio-related information strengthened or weakened the morphology–molecular correspondence.

4. RESULTS

4.1. Morphology and Types of Observed Trichomes

Across the six Solanaceae species, distinct trichome morphologies were observed per species. Considerable variation was identified in surface projections, overall structure, segmentation, and distribution pattern. Canescent, hispid, scabrous, and capitate trichomes were observed, and most of the observed trichomes were multicellular. In general, nonglandular trichomes were predominant. Figure 1 shows representative SEM images of trichomes from the six study species.

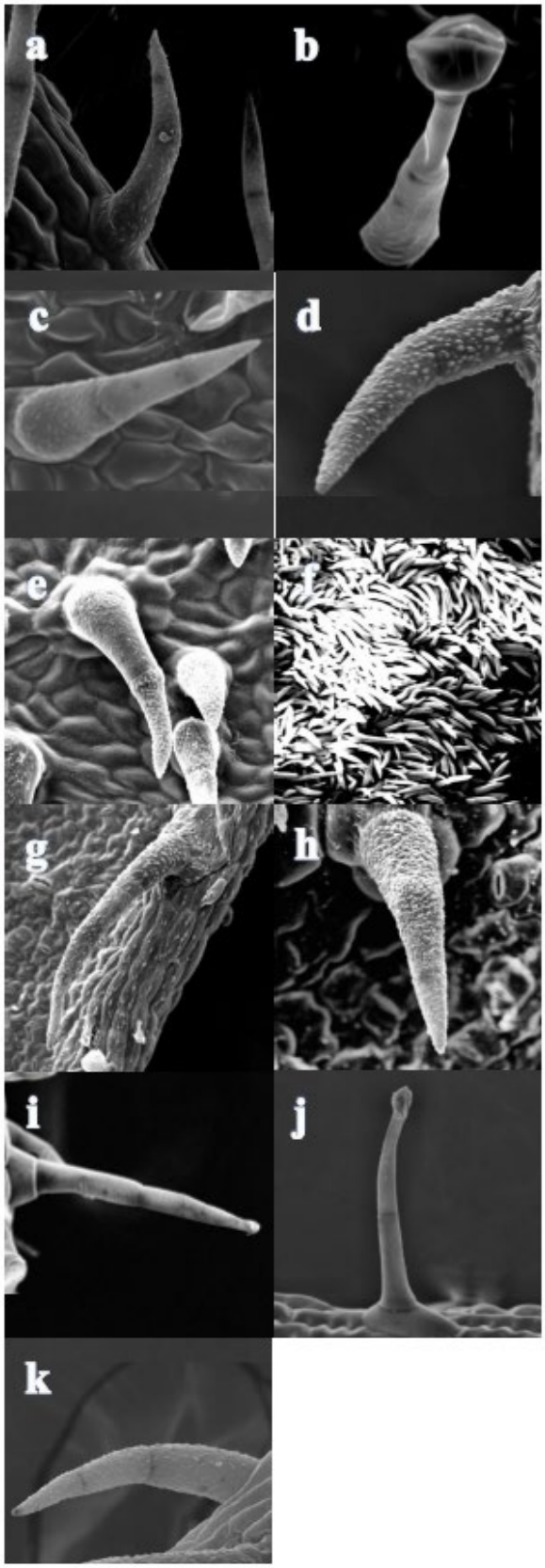

Figure 1. SEM Images of Trichomes in Six Solanaceae Species. (a–c) *Brugmansia suaveolens*; (d) *Capsicum annuum L.* var. grossum; (e–f) *Lycium chinense* Mill.; (g–h) *Physalis alkekengi L.* var. franchetii; (i–j) *Petunia* × *hybrida* 'Dreams Red'; (k) *Solanum nigrum* L. The images illustrate interspecific variation in overall structure, surface projections, segmentation, and distribution pattern.

4.2. Validation of the Focal Trait Block and Exclusion Logic

At the level of individual variables, the measured traits did not show a uniform statistical pattern. Most quantitative traits did not satisfy normality, and many showed interspecific differences in exploratory nonparametric testing. However, the focal trait block was not selected solely on the basis of univariate significance. Among the focal traits, Curvature per Length showed the strongest interspecific differentiation, whereas Tortuosity and Mean Curvature were less strongly supported as stand-alone variables. This indicates that focal trait selection should be interpreted at the level of a structurally complementary block rather than as a simple ranking of individually significant traits.

To evaluate the exclusion logic for non-focal variables, size-dominant descriptors were first examined as a group. A size-axis analysis showed that Area, Skeleton Length, Width (Max), Width (Tip), Length, Straight Length, Width (Base), Ellipse Major Axis, Perimeter, and Ellipse Minor Axis were strongly associated with a common size dimension. By contrast, Tortuosity and Mean Curvature were nearly independent of this size axis, whereas Curvature per Length showed an inverse relationship after length normalization. These results support the decision to prioritize path–curvature traits over size-dominant descriptors in the construction of the focal morphological distance matrix.

Redundancy among measured traits was also assessed. Strong pairwise redundancy was observed among several size-oriented variables, including Length versus Straight Length, Area versus Skeleton Length, and Perimeter versus Ellipse Major Axis. By contrast, the focal path–curvature traits were correlated but not interchangeable, indicating that they represented related yet non-identical aspects of structural organization.

At the block level, the focal trait block also showed significant multivariate species structure. PERMANOVA based on image-level median values yielded $F = 2.718$, $p = 0.009$, and $R^2 = 0.0787$. However, PERMDISP was also significant ($F = 2.330$, $p = 0.045$), indicating that part of the observed multivariate separation was influenced by among-group differences in dispersion as well as by differences in group centroids. Accordingly, the focal block was supported as informative but not as an exhaustively validated or uniquely optimal solution.

Taken together, these results strongly support the deprioritization of size-dominant descriptors, support the use of Contraction Ratio only in sensitivity analysis, and provide partial support for the exclusion of orientation-sensitive and local-extremum-based variables. The empirical basis for these decisions is summarized in Table 3 and Figure 2.

Table 3. Trait Selection and Exclusion Rationale. Summary of how measured trichome traits were prioritized or not prioritized in the present study. The table distinguishes between focal traits retained for the main analysis, traits retained only for sensitivity analysis, and trait groups that were not prioritized as focal descriptors. Validation status indicates whether the underlying rationale was strongly supported, moderately supported, or only partially supported under the current dataset.

Trait category	Decision in this study	Representative traits	Primary rationale	Empirical support in current dataset	Validation status
Focal path–curvature traits	Prioritized for main analysis	Tortuosity; Mean Curvature; Curvature per Length	Represents complementary dimensions of path deviation, overall bending, and length-normalized cumulative curvature	Exact Mantel significant (Spearman r_M = 0.775, p = 0.044); PERMANOVA F = 2.718, p = 0.009	Partially validated
Size-dominant descriptors	Not prioritized as focal traits	Area, Perimeter, Length, Straight Length, Width traits, Ellipse Major/Minor Axis, Skeleton Length	Likely to reflect overall scale more strongly than structural organization	Strong association with common size axis (ρ= 0.651–0.884)	Strongly supported
Orientation-sensitive descriptors	Not prioritized as focal traits	Bounding Box Aspect Ratio; Ellipse Angle	May vary with image orientation or projection in two-dimensional views	No direct image-rotation perturbation test performed; Ellipse Angle showed exploratory single-trait Mantel signal	Partially supported
Local-extremum / segment-dependent curvature descriptors	Not prioritized as focal traits	Max Curvature; Upper/Lower Curvature traits	Depend more strongly on local extrema or partial segments than on whole-axis structure	No direct segmentation-perturbation validation performed under current dataset	Partially supported
Contraction-related descriptor	Sensitivity analysis only	Contraction Ratio (as contraction ratio after |x| and log transform)	Combines directional and magnitude-related information; retained only to test robustness	Adding contraction_abs weakened correlation (Spearman r_M = 0.661, p = 0.086; Pearson r_M = 0.310, p = 0.572)	Supported
Skeleton-based ratio	Not prioritized as focal trait	Skeleton Ratio	Less direct structural interpretability and limited added value relative to focal path–curvature traits	Weak Kruskal–Wallis support (p = 0.268); weak single-trait Mantel (r_M = -0.257, p = 0.629)	Moderately supported

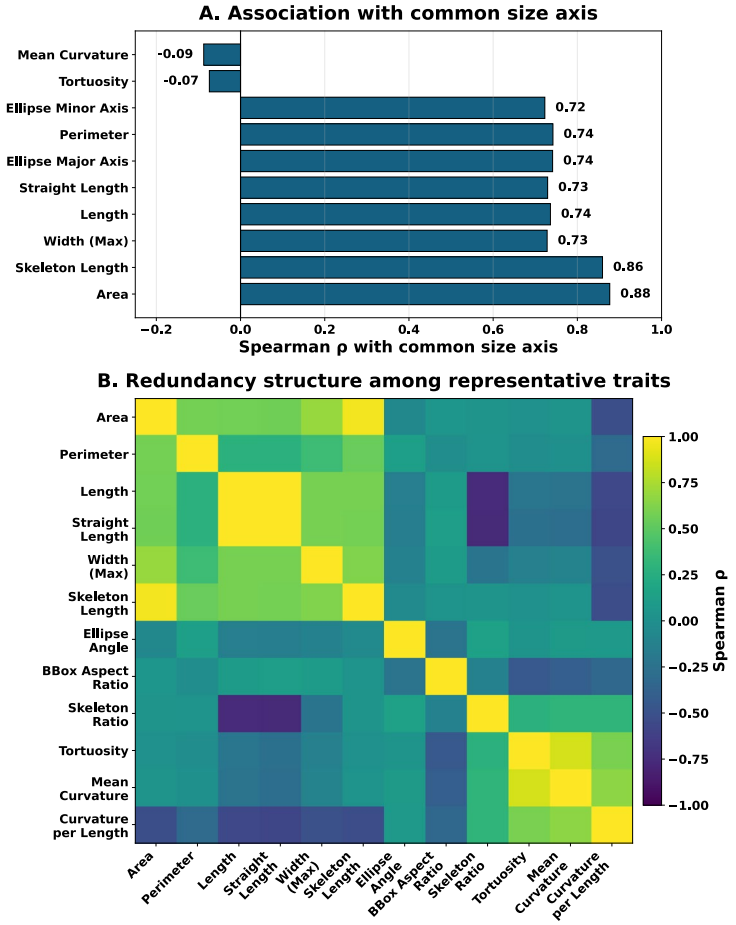

Figure 2. Trait Selection Validation for the Focal Path–Curvature Block. Panel A shows the association of representative candidate traits with the common size axis, illustrating the strong size dependence of excluded size-oriented descriptors and the relative size independence of the focal traits. Panel B shows the redundancy structure among representative measured traits based on Spearman correlation, highlighting strong redundancy among several size-dominant variables and partial complementarity among the focal path–curvature traits.

4.3. Morphospace Based on the Focal Trait Block

Morphological and molecular comparisons were conducted for six species: *Brugmansia suaveolens*, *Capsicum annuum* var. grossum, *Lycium chinense*, *Petunia* × *hybrida* 'Dreams Red', *Physalis alkekengi* var. franchetii, and *Solanum nigrum*. The focal trait block consisted of three quantitative variables: Tortuosity, Mean Curvature, and Curvature per Length.

After z-score standardization of these three traits, principal component analysis was performed using species-level centroids. PC1 explained 76.13% of the total variance and PC2 explained 23.14%, giving a cumulative explained variance of 99.27%. PC1 was primarily influenced by Tortuosity and Curvature per Length, whereas PC2 was most strongly influenced by Mean Curvature. These results indicate that interspecific variation within the focal trait block was structured mainly by path tortuosity, length-normalized curvature, and mean curvature.

However, the six species did not form completely discrete clusters in PCA space. *Brugmansia suaveolens* was relatively well separated from the other species along PC1, whereas the remaining five species occupied relatively adjacent regions. Therefore, the focal trait block organized the morphospace of the six Solanaceae species to a meaningful extent, but it did not allow clear species discrimination based solely on two-dimensional ordination. The PCA biplot is shown in Figure 3.

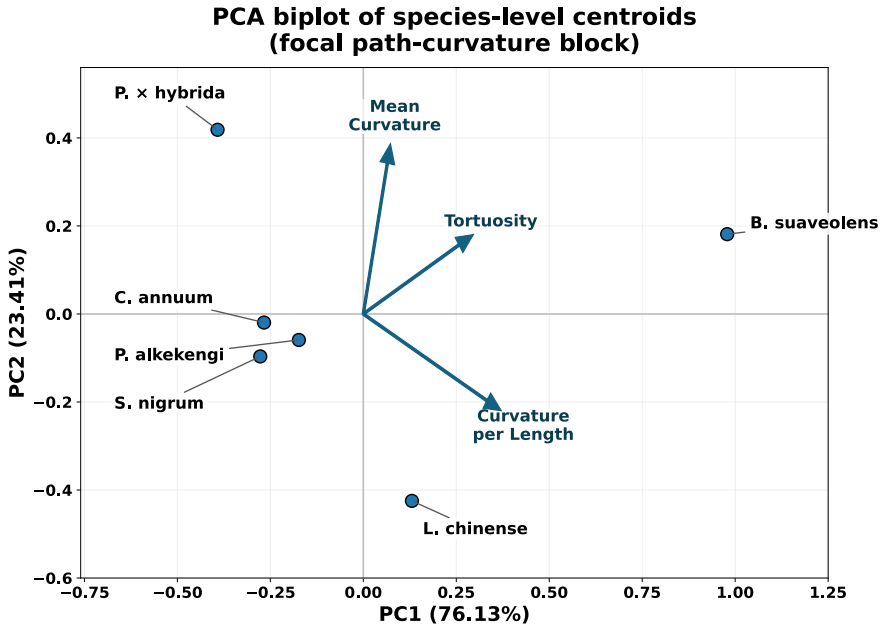

Figure 3. PCA Biplot of Species-Level Centroids Based on the Focal Trait Block in Six Solanaceae Species. PCA biplot of the species-level centroid matrix calculated from Tortuosity, Mean Curvature, and Curvature per Length. Arrows indicate the contribution and direction of each focal trait to the ordination space. Species positions represent relative differences in trichome path geometry and curvature among the six Solanaceae taxa.

4.4. Correspondence Between Morphological and Molecular Distance Matrices

Patristic distances calculated from the molecular phylogenetic tree showed that the molecularly closest pair was Capsicum annuum var. grossum and Solanum nigrum, with a molecular distance of 0.0176. The next closest pairs were *Lycium chinense* and *Physalis alkekengi* var. franchetii (0.0195), *Capsicum annuum var.* grossum and *Lycium chinense* (0.0203), and *Lycium chinense* and *Solanum nigrum* (0.0209). In contrast, *Brugmansia suaveolens* showed molecular distances ranging from 0.4518 to 0.4750 from all other species, indicating the greatest molecular divergence among the six taxa analyzed. The molecular phylogeny is shown in Figure 4.

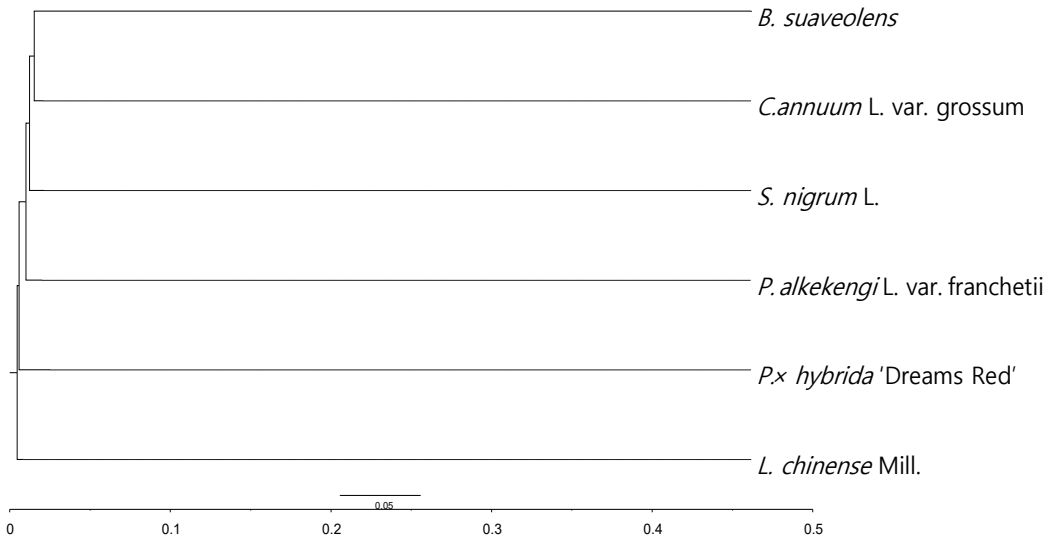

Figure 4. Molecular Phylogenetic Tree of Six Solanaceae Species Based on rbcL and matK Sequences. Molecular phylogenetic tree inferred from concatenated *rbcL* and *matK* sequences. Branch lengths are proportional to inferred genetic distance, and the topology was used to calculate patristic distances for construction of the molecular distance matrix. Where shown, node labels indicate branch support values from SH-aLRT and ultrafast bootstrap analyses.

The correlation between the morphological distance matrix and the molecular distance matrix was evaluated using the exact Mantel test. The Spearman exact Mantel test yielded r_M = 0.775 with p = 0.044. As a supplementary analysis, the Pearson exact Mantel test yielded r_M = 0.865 with p = 0.046. Thus, in these six Solanaceae species, the focal trait block composed of Tortuosity, Mean Curvature, and Curvature per Length showed a significant positive correspondence with molecular phylogenetic distance based on *rbcL* and *matK*. The numerical results are summarized in Table 4.

Comparison	Correlation coefficient	Exact p-value
Spearman exact Mantel	0.775	0.044
Pearson exact Mantel	0.865	0.046

Table 4. Exact Mantel Test Results Between the Morphological and Molecular Distance Matrices. Results of exact Mantel tests comparing the species-level morphological distance matrix with the molecular distance matrix derived from the *rbcL*- and *matK*-based phylogeny. The Spearman exact Mantel test was used as the primary inferential test, and the Pearson exact Mantel test was conducted as a supplementary analysis. r_M indicates the Mantel correlation coefficient.

These results indicate that, even though PCA did not show complete visual separation among species, the structure of the morphological distance matrix was not independent of the structure of the molecular distance matrix. Instead, both matrices varied in a concordant direction. This correspondence is further illustrated in the heatmap comparison presented in Figure 5.

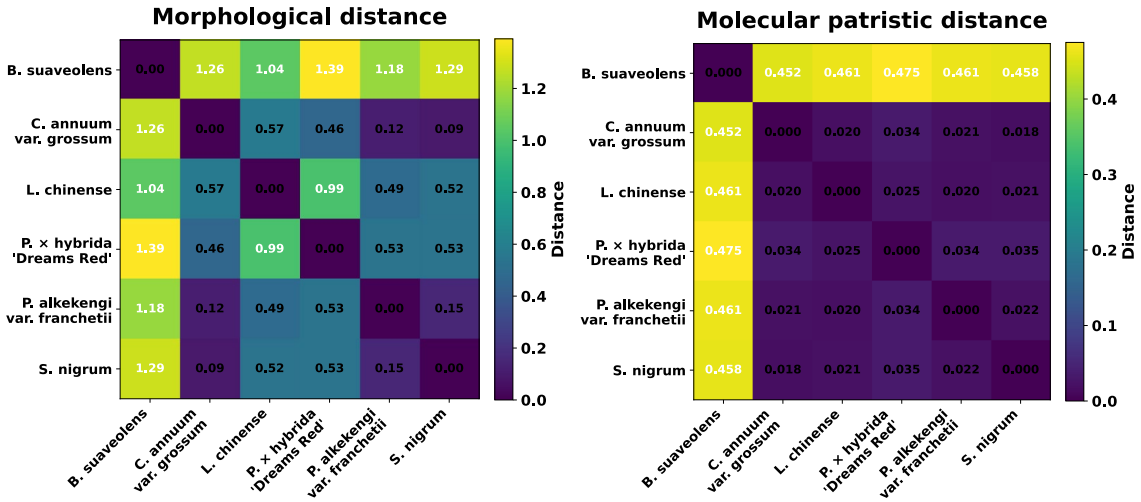

Figure 5. Heatmap Representations of the Morphological and Molecular Distance Matrices for Six Solanaceae Species. Side-by-side heatmaps of the species-level morphological distance matrix and the molecular distance matrix. The heatmaps visualize the overall structure of pairwise interspecific distances and provide a qualitative comparison of the extent to which morphological distances correspond to molecular phylogenetic distances.

4.5. Sensitivity Analysis

To evaluate the structural stability of the main result, a leave-one-species-out sensitivity analysis was performed. Overall, the tendency toward positive correspondence was retained across reduced five-species datasets, but the strength of the correlation varied depending on which species was excluded.

When Brugmansia suaveolens was excluded, the Spearman exact Mantel correlation coefficient decreased to 0.333 and the p-value increased to 0.575, indicating a loss of statistical significance. In contrast, when *Lycium chinense* was excluded, the highest correlation was observed, with r_M = 0.927 and p = 0.042. The remaining leave-one-species-out results were as follows: excluding *Petunia* × *hybrida* 'Dreams Red' yielded r_M = 0.709 and p = 0.100; excluding *Solanum nigrum* yielded r_M = 0.733 and p = 0.117; excluding *Physalis alkekengi* var.

franchetii yielded r_M = 0.806 and p = 0.067; and excluding *Capsicum annuum var*. grossum yielded r_M = 0.879 and p = 0.050. These results indicate that the observed morphology–molecular correspondence was not distributed uniformly across all taxa, but was strengthened by the relative position of particular species within the distance structure. The full numerical results are summarized in Table 5, and the leave-one-species-out pattern is visualized in Figure 6.

analysis	Excluded species	type	r_M	p-value
LSO	*B. suaveolens*	Spearman	0.333	0.575
LSO	*P.* × *hybrida* 'Dreams Red'	Spearman	0.709	0.100
LSO	*S. nigrum*	Spearman	0.733	0.117
LSO	*P. alkekengi* var. *franchetii*	Spearman	0.806	0.067
LSO	*C. annuum* var. *grossum*	Spearman	0.879	0.050
LSO	*L. chinense*	Spearman	0.927	0.042
TBA	Main focal block	Spearman	0.775	0.044
TBA	Main focal block	Pearson	0.865	0.046
TBA	Focal block + contraction ratio	Spearman	0.661	0.086
TBA	Focal block + contraction ratio	Pearson	0.310	0.572

Table 5. Sensitivity Analyses of the Focal Trait Block. Summary of robustness checks for the focal path–curvature trait block. Leave-one-species-out analyses were used to evaluate dependence on species composition, and block augmentation with contraction ratio was used to assess whether Contraction Ratio–related information strengthened or weakened morphology–molecular correspondence.

In the table, Leave-one-species-out is denoted as LSO and Trait-block augmentation as TBA.

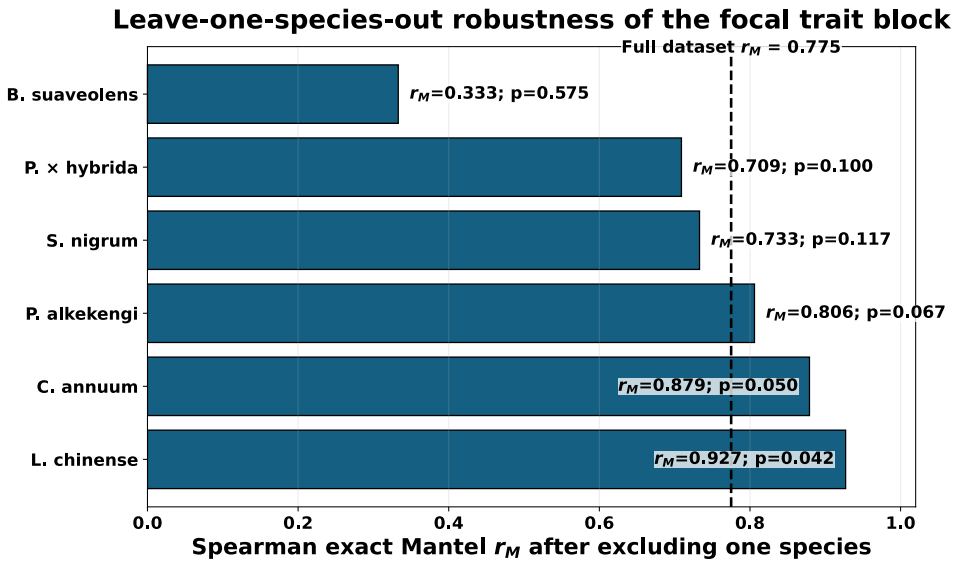

Figure 6. Leave-One-Species-Out Robustness of the Focal Trait Block. Horizontal bar plot of Spearman exact Mantel correlation coefficients obtained after excluding one species at a time. The dashed vertical line indicates the full-dataset exact Mantel correlation (r_M = 0.775), allowing direct comparison between the main result and the reduced-data sensitivity analyses.

A second sensitivity analysis was conducted by defining contraction_abs as the absolute value of Contraction Ratio followed by log transformation and then adding this variable to the focal trait block. Under this expanded trait block, the Spearman exact Mantel test yielded r_M = 0.661 with p = 0.086, and the Pearson exact Mantel test yielded r_M= 0.310 with p = 0.572. Thus, the inclusion of Contraction Ratio-related information weakened rather than strengthened the morphology–molecular correspondence. This result indicates that the core signal detected in this study was more clearly captured by the original focal trait block than by the addition of Contraction Ratio-derived information.

5. DISCUSSION

5.1. Implications of Morphological–Molecular Correspondence

The most important result of this study is that, in the six Solanaceae species examined, the focal trait block composed of Tortuosity, Mean Curvature, and Curvature per Length showed significant positive correspondence with interspecific molecular phylogenetic distance based on *rbcL* and *matK*. Within the scope of the present analysis, this indicates that structural differences in trichome morphology are not merely arbitrary interspecific variation, but vary in a direction that is concordant with the distance structure of the molecular phylogeny.

At the same time, this signal should be interpreted cautiously. The present study supports a significant matrix-level correspondence between morphology and molecular phylogeny, but it does not demonstrate a robust and fully stable morphology-based phylogenetic classification system. In other words, the results indicate a limited but non-trivial phylogenetic signal rather than a complete topology-level reconstruction of evolutionary relationships.

This distinction is important. The present study does not argue that trichome morphology as a whole is uniformly phylogenetically informative. Rather, it suggests that under the current sampling scheme and analytical design, a specific focal block of path–curvature-related traits captures a detectable component of phylogenetically relevant variation.

5.2. Why the Focal Path–Curvature Trait Block Was Prioritized

The focal traits selected in this study—Tortuosity, Mean Curvature, and Curvature per Length—were not prioritized simply because they produced the strongest individual p-values. Instead, they were prioritized because they jointly represent complementary aspects of structural organization, namely path deviation, overall bending, and length-normalized cumulative curvature.

The strongest empirical support for this prioritization comes from the reduced dominance of absolute size. Size-oriented descriptors such as Area, Perimeter, Length, Straight Length, Width-based variables, Ellipse Major Axis, Ellipse Minor Axis, and Skeleton Length were strongly associated with a common size axis, whereas Tortuosity and Mean Curvature were nearly independent of that axis and Curvature per Length was reduced in size dependence through normalization by length. In this sense, the focal block was less strongly driven by overall scale than many of the excluded descriptors.

The present study also showed that several excluded size-related traits were highly redundant with one another. By contrast, the focal path–curvature traits were correlated but not fully interchangeable, indicating that they retained partially distinct structural information when used as a block.

However, the exclusion logic was not equally validated for all non-focal variables. The deprioritization of size-dominant descriptors and the use of Contraction Ratio only in sensitivity analysis were relatively well supported under the current dataset. By contrast, the deprioritization of orientation-sensitive variables such as Bounding Box Aspect Ratio and Ellipse Angle, and of local-extremum or segment-dependent variables such as Max Curvature and Upper/Lower Curvature traits, remains only partially validated because explicit image-based perturbation tests were not performed. Likewise, Skeleton Ratio appeared less directly interpretable and less useful for the focal matrix-level comparison, but its exclusion should be viewed more cautiously than that of the clearly size-dominant variables.

Taken together, the focal block should not be interpreted as a uniquely proven optimum among all possible trait combinations. Rather, it should be interpreted as a structurally interpretable and partially validated block that performed plausibly and consistently enough to justify matrix-level testing against molecular phylogenetic distance.

5.3. Why PCA Did Not Show Clear Clusters While the Mantel Test Was Significant

In this study, PCA did not separate the six species into completely distinct clusters. In particular, Brugmansia suaveolens was relatively well separated, whereas the remaining five species partially overlapped or occupied

nearby positions. Superficially, such a result could give the impression that trichome morphology does not provide clear taxonomic separation.

However, this does not contradict the central finding of the study, because PCA and the Mantel test answer fundamentally different questions. PCA is a descriptive visualization tool that projects high-dimensional data into a lower-dimensional space and is useful for intuitively examining how cleanly taxa appear to separate. It is not, however, a formal method for testing correspondence between two distance matrices. By contrast, the Mantel test compares the full matrix of pairwise distances among all species pairs and is therefore more appropriate for evaluating overall structural correspondence between two distance systems.

Therefore, the absence of complete cluster separation in PCA does not imply the absence of phylogenetic signal in trichome morphology. Rather, it indicates that the signal is expressed more clearly as matrix-level correspondence in interspecific distance structure than as categorical visual separation in two-dimensional ordination space. The significant Mantel correlation despite overlapping PCA clusters suggests that the phylogenetic signal resides in the relative spacing of taxa in the morphospace rather than in the existence of discrete, well-separated morphological gaps. This supports the methodological choice made in the present study to treat the exact Mantel test as the primary inferential framework. Given the small sample size of six species, the use of exact permutation based on all possible label rearrangements was especially appropriate because it provides a more conservative and rigorous significance assessment than approximate randomization.

5.4. Interpretation of Species Influence and Structural Fragility of the Signal

The sensitivity analysis showed that the morphology–molecular correspondence detected in this study is not yet a fully stable pattern. In particular, when Brugmansia suaveolens was excluded, the Spearman exact Mantel correlation coefficient declined to 0.333 and statistical significance disappeared. This indicates that the current signal is strengthened to a substantial extent by the relative position of particular taxa within the distance structure.

This finding may be interpreted in two ways. First, Brugmansia suaveolens occupied a relatively distinct position both in the molecular phylogeny and in the trichome morphospace. Its inclusion may therefore have expanded the range of both the morphological and molecular distance matrices, making morphology–molecular correspondence more apparent. Second, the current focal trait block may be more sensitive to deeper phylogenetic divergence than to finer-scale differences among closely related taxa.

A supplementary topology check based on hierarchical clustering further supports this cautious interpretation. Internal bootstrap support values were generally low, indicating that the morphology-based branching order was not strongly stable under resampling. This suggests that the present signal is better interpreted as a limited distance-level correspondence than as a robust tree-like topology reconstructed from morphology alone.

Accordingly, the results of the present study should not be generalized too broadly. The study is meaningful in showing that phylogenetic signal can be detected in Solanaceae trichome morphology, but it does not justify the stronger claim that a robust morphology-based phylogenetic classification system has already been established. Rather, the present findings should be interpreted as identifying a promising but still fragile focal signal, expressed mainly at the level of matrix correspondence and possibly strengthened by deeper phylogenetic divergence within the current six-species dataset.

This pattern may be interpreted as a possible deep-split signal rather than as uniform species-level resolution. In other words, the focal path–curvature block may capture morphological differentiation more clearly when phylogenetic divergence is relatively large, whereas finer-scale differences among more closely related Solanaceae taxa may be weaker or more easily obscured by developmental variation, environmental effects, individual-level variation, and measurement noise. Under this interpretation, the disappearance of statistical significance after excluding B. suaveolens does not simply invalidate the result; rather, it suggests that the present six-species dataset may be more informative about deeper phylogenetic divergence than about shallow within-family or within-genus differentiation. This interpretation remains a hypothesis, however, and should be tested through expanded within-genus sampling.

5.5. Scientific Meaning and Future Direction

The significance of this study does not lie only in the fact that a particular trait block was statistically significant. More importantly, the study clarifies what kind of analytical framework is appropriate when interpreting trichome morphology from a phylogenetic perspective. Multiple quantitative traits were measured, and a focal trait block was then prioritized on the basis of structural interpretability, reduced size dominance, limited redundancy among core dimensions, and suitability for matrix-level comparison. At the same time, the study also makes clear that not all exclusion criteria were equally validated under the current dataset.

In addition, the study distinguished between the role of visualization methods and the role of inferential tests, and interpreted the results primarily through the exact Mantel test. In this way, it provides a clearer statistical framework for the interpretation of morphological data, while also indicating where additional validation remains necessary.

This also leads naturally to future research directions. First, within-genus sampling will be necessary in order to test whether the observed signal is strongest at deeper phylogenetic splits or whether it is retained among more closely related lineages. Second, future work should move beyond species-centroid comparison and adopt biological replicate-based designs that distinguish independent individuals, developmental stages of leaves, and sampling positions. Third, the inclusion of spatial traits such as trichome density, nearest-neighbor distance, and pattern regularity may allow assessment not only of individual trichome shape but also of the structural organization of the entire leaf surface. Fourth, image-based perturbation tests, including rotation and segmentation-stability analyses, will be necessary to validate more rigorously the exclusion logic for orientation-sensitive and local-extremum-based descriptors. Fifth, integration with molecular developmental or functional data will be necessary to determine how the observed morphological differences are related to underlying developmental mechanisms.

Taken together, the present study is less a final endpoint than a methodological stepping stone toward more rigorous hypothesis-driven research on Solanaceae trichomes. It is precisely in this sense that the study has independent scientific value.

6. CONCLUSION AND SUGGESTIONS

6.1. Conclusion

This study measured multiple quantitative trichome traits in six Solanaceae species and evaluated the correspondence between a morphological distance matrix and a molecular distance matrix derived from an *rbcL*- and *matK*-based phylogeny, with emphasis on a focal trait block representing structural path geometry and curvature. The focal trait block composed of Tortuosity, Mean Curvature, and Curvature per Length showed significant positive correlation with molecular phylogenetic distance in the exact Mantel test (Spearman exact Mantel: r_M = 0.775, p = 0.044; Pearson exact Mantel: r_M = 0.865, p = 0.046). These findings suggest that trichome morphology in Solanaceae is not merely a superficial or random source of variation, but may, at least in part, reflect phylogenetically relevant differentiation.

The study also indicates that trichome morphology should not be interpreted only in terms of size or count-based descriptors. Instead, structural organization in terms of path geometry and curvature may be more informative for detecting phylogenetically meaningful variation. Under the current dataset, the deprioritization of size-dominant descriptors and the use of Contraction Ratio only in sensitivity analysis were comparatively well supported, whereas the exclusion of orientation-sensitive and local-extremum-based descriptors remains only partially validated and should therefore be interpreted more cautiously.

At the same time, the present study revealed clear limitations. PCA did not produce complete visual separation among the six species, sensitivity analyses showed marked dependence on species composition, and supplementary topology checks indicated low internal bootstrap stability. Therefore, the results should not be interpreted as demonstrating that a robust morphology-based phylogenetic classification system has already been established for Solanaceae trichomes. Rather, the present study identifies a partially validated focal trait block that captures a limited but significant matrix-level phylogenetic signal.

In this sense, the principal contribution of the study lies not in claiming definitive proof of trichome-based phylogenetic reconstruction, but in showing which kinds of traits, interpreted under which analytical framework, can yield meaningful evidence of morphology–molecular correspondence.

6.2. Suggestions

First, broader taxon sampling within Solanaceae, especially the inclusion of multiple species within the same genus, will be necessary to validate the present findings more robustly. Such sampling would directly test the deep-split hypothesis suggested by the present sensitivity analysis, namely whether the focal path–curvature trait block is informative mainly at deeper phylogenetic divergences or whether it also retains detectable signal at shallower within-genus scales.

Second, because the present analysis relied on species-level centroid values, future research should adopt a biological replicate-based design with increased numbers of independent individuals and clearer control of leaf developmental stage and sampling position. This will be necessary to distinguish whether the observed morphological variation reflects relatively stable species-level properties or whether it is strongly influenced by development or microenvironment.

Third, future studies should extend the focal trait set beyond path–curvature traits to include spatial variables such as trichome density, distribution, nearest-neighbor distance, and pattern regularity. Such traits may capture organizational properties of the leaf surface that cannot be explained by the morphology of individual trichomes alone and may therefore provide additional phylogenetic signal.

Fourth, explicit image-based perturbation tests should be incorporated in future work. Rotation tests, segmentation-stability analyses, and local trimming or smoothing perturbations would make it possible to evaluate more rigorously whether orientation-sensitive and local-extremum-based descriptors should indeed be deprioritized in morphology–phylogeny studies.

Fifth, it will be important to integrate trichome morphology with developmental genetic or functional data. Such integration may clarify how the observed morphological differences are related to underlying biological mechanisms and may extend the interpretation of morphology–molecular correspondence beyond a simple correlational framework toward developmental and evolutionary explanation.

7. REFERENCES

[1] S. Watts and R. Kariyat, “Morphological characterization of trichomes shows enormous variation in shape, density and dimensions across the leaves of 14 Solanum species,” *AoB Plants*, vol. 13, no. 6, Art. no. plab071, 2021, doi: 10.1093/aobpla/plab071.

[2] H.-J. Ensikat, H. Wessely, M. Engeser, and M. Weigend, “Distribution, ecology, chemistry and toxicology of plant stinging hairs,” *Toxins*, vol. 13, no. 2, Art. no. 141, 2021, doi: 10.3390/toxins13020141.

[3] W. S. Judd, C. S. Campbell, E. A. Kellogg, P. F. Stevens, and M. J. Donoghue, *Plant Systematics: A Phylogenetic Approach*, 3rd ed. Sunderland, MA, USA: Sinauer Associates, 2007.

[4] A.-K. Aschenbrenner, S. Horakh, and O. Spring, “Linear glandular trichomes of Helianthus (Asteraceae): Morphology, localization, metabolite activity and occurrence,” *AoB Plants*, vol. 5, Art. no. plt028, 2013, doi: 10.1093/aobpla/plt028.

[5] N. Mantel, “The detection of disease clustering and a generalized regression approach,” *Cancer Research*, vol. 27, no. 2, pp. 209–220, 1967.

[6] L. A. Urry, M. L. Cain, S. A. Wasserman, P. V. Minorsky, and R. B. Orr, *Campbell Biology*, 12th ed. New York, NY, USA: Pearson, 2021.

[7] P. M. Hollingsworth, S. W. Graham, and D. P. Little, “Choosing and using a plant DNA barcode,” *PLOS ONE*, vol. 6, no. 5, Art. no. e19254, 2011, doi: 10.1371/journal.pone.0019254.